EXPERIMENTAL INVESTIGATION OF THERMO- AND FLUIDDYNAMICS IN A HORIZONTAL EVAPORATOR TUBE WITH INJECTION

K. Laufs, F. Mayinger

Lehrstuhl A für Thermodynamik
Technische Universität München, Germany

ABSTRACT

Measurements of heat transfer rates and flow patterns in a horizontal evaporator tube are conducted. Flow conditions were such, that gravitational forces dominated, causing the liquid to be collected in the bottom of the tube. Shear forces let a liquid film spread on the circumference to a certain degree. Usually the liquid and the vapor phases are completely segragated. Thus a simple model, that divides the inside of the tube surface into a wetted and a dry area, can be applied. Heat transfer rates in the wetted area may be described by convective flow boiling correlations and heat transfer rates in the dry area by post-dryout heat transfer correlations, both known from literature. Wetting angles were measured in the range from 90 to 150 deg. Three heating profiles were investigated, namely heating of the bottom half, of one side half and of the total circumference of the tube uniformly. The heating profile was found to be crucial for the arising temperature distribution in the tube wall. When either one side or the total circumference is heated, high temperature differences occur.

1. INTRODUCTION

Steam generation in absorber tubes of solar parabolic troughs needs high qualities of the steam/water-mixture to avoid flow instabilities and damage by slugs. This operational condition can be achieved by stepwise injecting water along the evaporator tube. An initial steam flow must be provided.

Gravity forces collect the liquid in the lower part of the tube and friction forces generated by the slip between the vapor and the liquid can cause a spreading of the liquid around the circumference of the tube wall especially at high vapor velocities. When the flow is stratified, a significant portion on the upper circumference of the tube surface may be continously dry. Furthermore, when vapor velocities are low, a high degree of phase separation is likely to occur. Under these circumstances the prevailing heat transfer mechanisms from the inside tube surface to the fluid may be described separately for the wetted and for the dry region, namely convective flow boiling in the wetted and post-dryout heat transfer in the dry region.

Numerous flow boiling correlations for evaporation in horizontal tubes are known from literature. Most of the correlations predict large databases with mean accuracies of 20-30%, with many datasets off by much more (Thome [1]). An empirical correlation is given, for example, by Gungor [2]:

$$h_{2ph} = Eh_l + Sh_{pool}\,. \tag{1}$$

h_l is given by the Dittus-Boelter equation

$$h_l = \frac{\lambda_l}{d} 0.023 Re_l^{0.8} Pr_l^{0.4}\,. \tag{2}$$

Gungor evaluates the pool boiling coefficient by

$$h_{pool} = 55 p_r^{0.12} (-\log_{10} p_r)^{-0.55} M^{-0.5} \dot{q}^{0.67} \tag{3}$$

and S is the boiling suppression factor

$$S = \frac{1}{1 + 1.15 \cdot 10^{-6} E^2 Re_l^{1.17}} . \quad (5)$$

According to Thome, though, a fully descriptive model should take stratification and non-equilibrium effects, thus the influence of a partly dry wall, into account.

Especially in the beginning of the evaporation path of a solar evaporator, stratification of the flow is expected. Depending on the heating profile (the heating profile changes from morning to noon and evening) and vapor velocity, critical situations in the cooling of the upper portion of the tube wall may occur. The experiments were carried out with special interest to these conditions. Fig. 1 shows the flow regimes of the experiments calculated according to the Taitel & Dukler [3] flow regime map. The figure indicates the stratified flow regime for all experiments, some being close to the boundary of annular flow.

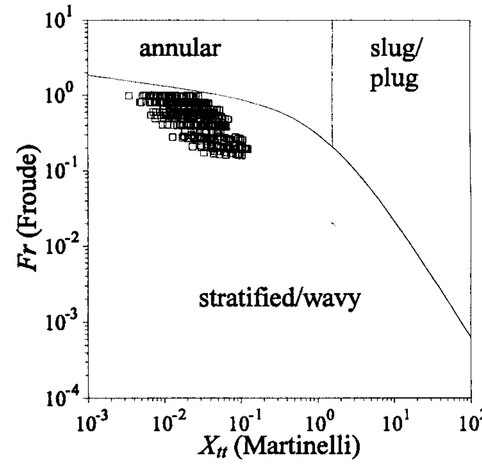

Fig. 1: Flow regimes of experiments acc. to Taitel & Dukler

2. DESCRIPTION OF EXPERIMENT

Experiments were carried out in a 8 m long test tube with an inner diameter of 64 mm. A test loop (fig. 2) was built to generate vapor and liquid mass flow rates in a wide range of parameters, so that almost any history of 2-phase flow situations being expected in a very long solar evaporator could be simulated. Instead of water Freon 11 was used as modeling fluid. Table 1 shows the test parameters and their variation. The injection mass flow rate is adjusted in such a way, that the amount of injected liquid is evaporated totally by the end of the distance between injectors.

parameter	unit	Freon 11	water equivalent
pressure	bar	4.6/9.6/16.7	30/60/100
mass flux	kg/m²s	45/90/135/180/225	50/100/150/200/250
heat flux	kW/m²	1.3/2.6/3.9/5.25	19/37/56/75
distance between injectors	m	10/20/30/60	
heating profile		bottom/side/uniformly	

Table 1: Test parameters

Three different cases of heating the tube wall were examined to simulate the heat addition by solar radiation, namely electrically heating 1) the lower half of the tube only, corresponding to operation at noon, 2) on one side, corresponding to operation in the morning/evening and 3) for reference purposes the total circumference uniformly.

The test tube was designed in such a way, that flow pattern and wetted areas could be observed by optical means. In addition, the void fraction and to a certain extent also the void distribution could be measured with a capacitive sensor. The outer tube wall was instrumented with thermocouples. Furthermore, the superheating of the vapor and by this the thermodynamic non-equilibrium in the tube could be monitored with special thermocouples. See fig. 2 for details of the instrumentation.

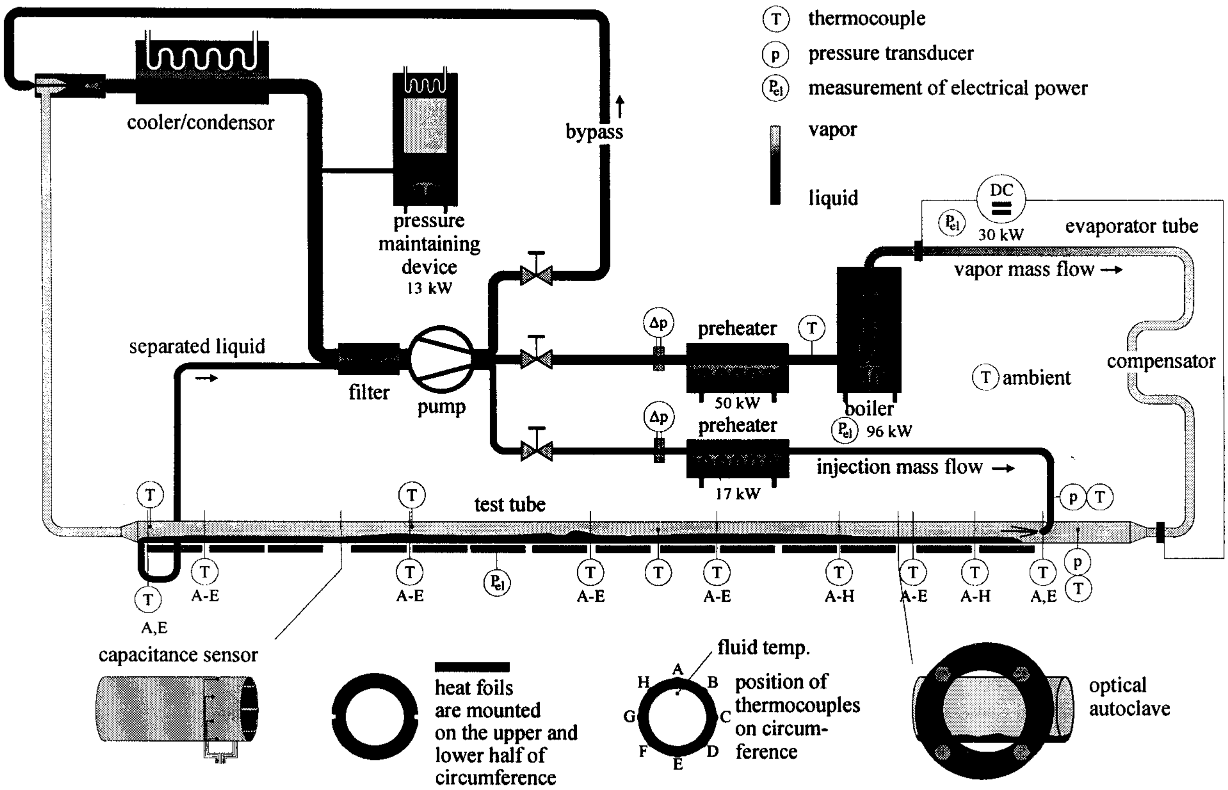

Fig. 2: Test loop and instrumentation of test tube

3. MEASUREMENT AND EVALUATION TECHNIQUES

Temperatures were measured on the circumference of the outer tube wall at several positions along the test tube. For every cross-section calculations were performed to obtain the temperature distribution. The calculation code solves the heat conductance equations in radial and circumferential directions using a ADI-method. On the outside boundary the conditions are given - the heating profile by default and the heat flux by measurement data. On the inside boundary a simple model is used, where the circumference is splitted into a dry and a wetted area, each having a own, uniform heat transfer coefficient. Of course, the wetted angle and the heat transfer coefficients are unknowns. They are obtained iteratively until the calculated temperature profile perfectly fits the measured temperatures (see fig. 5). For almost all of the performed calculations a unique combination of wetted angle and heat transfer coefficients exists, because the temperature distribution is very sensitive to a change in one of these parameters. Typical accuracies are ±2° for the wetted angle, ± 5° W/m²K for the heat transfer coefficient in the dry area and ± 50 W/m²K for the heat transfer coefficient in the wetted area.

The calculation code also takes into account the vapor superheat temperature, which is measured in the top of the tube (see fig. 2 fluid temp.). Herbst *et al.* [4] measured the thermal stratification of the fluid flow inside a tube. According to their experimental results a linear thermal stratification of the vapor flow is assumed, when the total circumference or one side of the tube is heated, whereas a constant vapor temperature is assumed, when the bottom half is heated.

The capacitance measurement technique is described by Klug [5]. A 8-electrodes non-invasive sensor was designed to meet the high temperature (up to 200°C) and pressure (up to 25 bars) requirements. Calibration measurements were made simulating ideal stratified flows, annular and semi-annular flows. Special calibration measurements were made to compensate for the temperature drift. A multiplexer was designed, capable of generating any electric field within the 8 electrodes. Extraordinary efforts were undertaken to minimize stray capacities around the sensor and inside the multiplexer.

The optical autoclave was designed to allow for a lateral view of the flow without disturbing it. It has a glass tube inside and flat glasses outside that withstand the pressure. The autoclave is heated externally in order to generate slightly superheated vapor in the space between the glasses and thus guarantee a clear view.

4. RESULTS AND DISCUSSION

The temperature distribution inside the tube wall, especially in the circumferential direction, is mainly a function of geometry - the wetted angle on the inside tube surface and the heating profile corresponding to solar radiation conditions on the outside tube surface (fig. 4 + 5). In the dry area the vapor is heated via single-phase heat transfer directly from the tube wall, resulting in superheated vapor. The more heat is transferred to the dry area, the higher are vapor and wall temperatures in this area. On the other hand the wetted area is always cooled well. Figures 4 + 5 also indicate, that remarkably high heat flows exist in circumferential directions, which are diverted into the liquid at the edges of the wetted area.

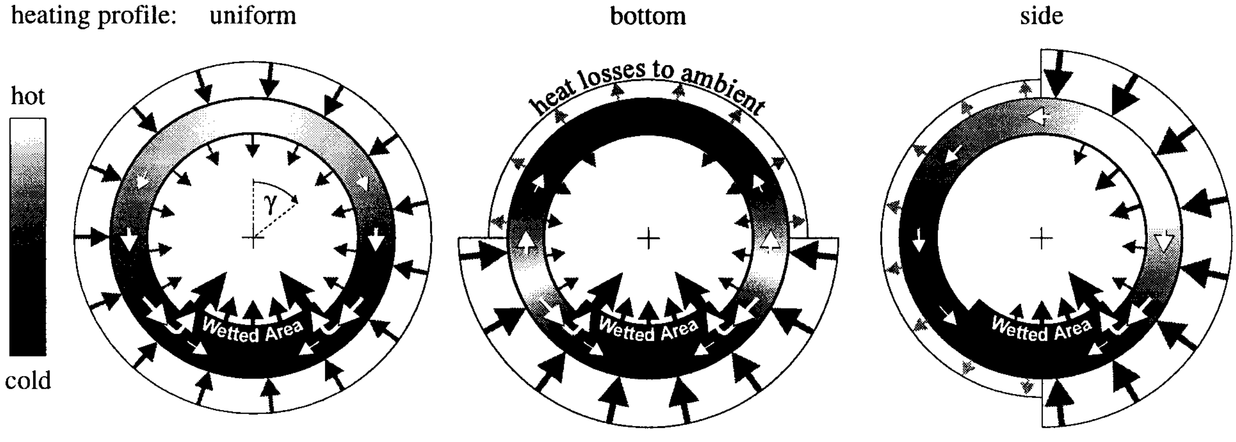

Fig. 4: Heat flows for the 3 investigated heating profiles.

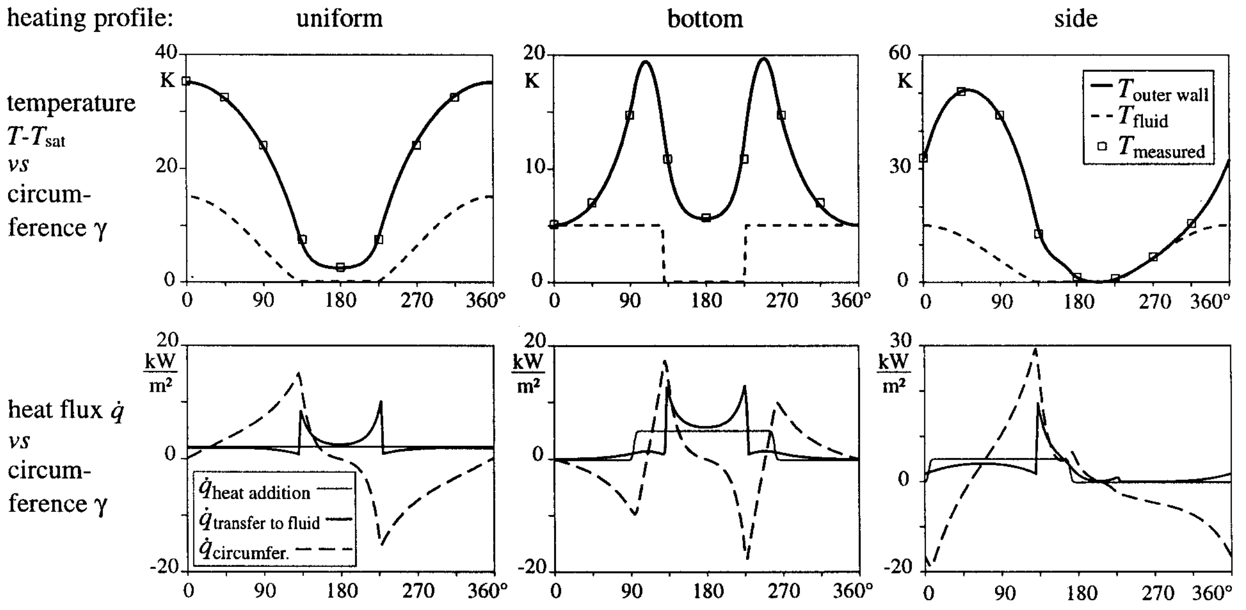

Fig. 5: Sample calculation results · Total heat addition, wetted angle and heat transfer coefficients h_{dry} and h_{wet} are the same for the 3 heating profiles. Typical vapor superheat temperatures were chosen.

On photographs (for example fig. 6) the observed flow patterns were found to be as expected (fig. 7). Except for the lowest mass flux rate (50 kg/m²s) a partially spreading of a liquid film around the circumference was observed for all flow conditions. This is in agreement with the measured wetted angles, which were in the range from 90° to 150°. If an ideal stratification were assumed, the wetted angles would have ranged between 20° and 50° only.

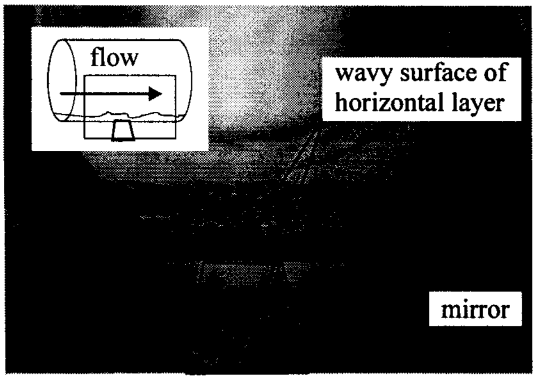

Fig. 6: Stratified flow at low mass flux

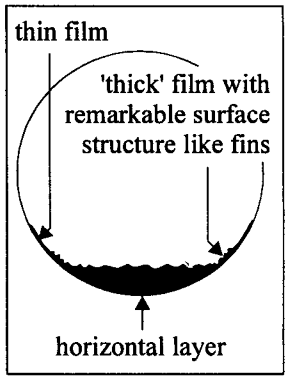

Fig. 7: Flow pattern

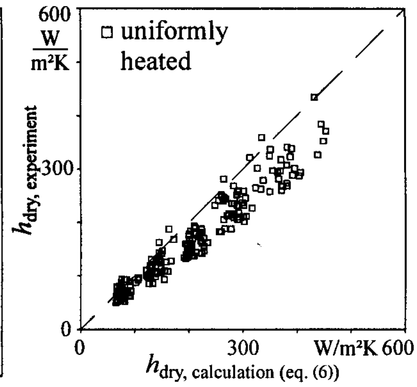

Fig. 8: $h_{\text{dry area}}$ (exp. *vs* calc.)

From the capacitance data a high liquid holdup was detected. This was expected, because at low vapor velocities the friction forces of the vapor at the phase interface are not strong enough to drive the liquid through the tube with an appropriate velocity. In some cases the liquid accumulated such, that the flow began to form surge/slug-like waves (observed on photos).

The measured heat transfer coefficients of the wetted area were plotted against values calculated from the Gungor equations (1)-(5). The mean deviation of all the data points was 34%, which is satisfactory, as Gungor himself reports accuracies of 20% to 50% for different fluids and databases. Furthermore, the Gungor equation gives an overall heat transfer coefficient, whereas in our approach the flow boiling heat transfer coefficient is referred to the wetted area only. Note, that the exact value for the flow boiling heat transfer coefficient is not crucial for the arising temperature distribution in the tube wall.

The heat transfer coefficients for the dry area, obtained from the uniformly heating measurements, follow the single-phase convective heat transfer correlation of Gnielinski [6]:

$$h_v = \frac{\lambda_v}{d} \frac{(\xi/8)(Re_v - 1000)Pr_v}{1 + 12{,}7\sqrt{(\xi/8)}(Pr_v^{2/3} - 1)}, \tag{6}$$

where the hydraulic diameter d is referred to the measured dry area (fig. 8).

When heating the tube either uniformly or on one side, high superheating of the vapor was observed. The following empirical correlation for the ratio of equilibrium to actual quality $k_{vs} = \dot{x}_{eq} / \dot{x}_{act}$ fits our experimental data best (fig. 9 + 10):

$$k_{vs,\text{ max., uniformly h.}} = 2600 \cdot Re_v^{-0.8} Pr_v^{1.4} \cdot \tanh\left(3.5 \frac{\dot{x}_{eq} - \dot{x}_{inj}}{1 - \dot{x}_{inj}}\right) + 1 \tag{7}$$

Note, that the higher the vapor and the wall's dry area temperatures are, the more heat is transferred circumferentially via conductance to the well cooled wet area, and the less heat is transferred via convection to the vapor flow. Rising vapor and wall's dry area temperatures thus cause a shift in the tube's inside heat flow balance, which is indicated by the flattening slope of k_{vs} with increasing $\dot{x}_{eq}$ (fig. 10).

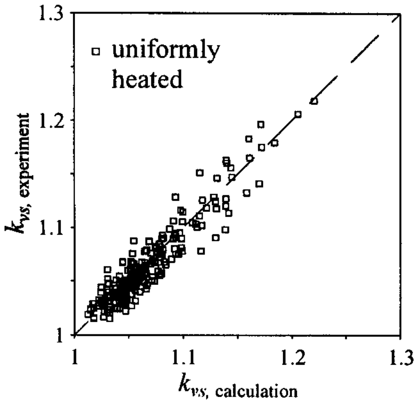

Fig. 9: k_{vs} (experiment *vs* calculation)

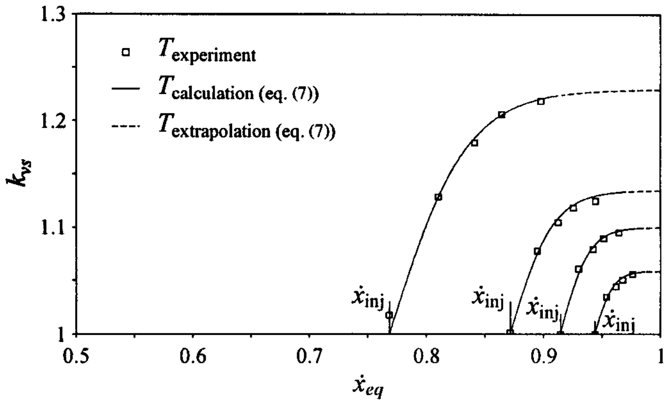

Fig. 10: Sample data k_{vs} *vs* $\dot x_{eq}$

5. NOMENCLATURE

Bo	-	boiling number $Bo = \dot q / (\dot m h_{vl})$	Re_l	-	Reynolds no. $Re_l = d\dot m(1-\dot x)/\eta_l$
d	m	diameter	Re_v	-	Reynolds no. $Re_v = d\dot m \dot x / \eta_v$
E	-	2-phase enhancement factor	$\dot x$	-	vapor quality
Fr	-	Froude no. $Fr = \dot x \dot m \left(gd(\rho_l - \rho_v)\rho_v\right)^{-0.5}$	S	-	boiling suppression factor
g	m/s^2	gravitational acceleration	X_{tt}	-	Martinelli parameter
h	W/m^2K	heat transfer coefficient			$X_{tt} = ((1-\dot x)/\dot x)^{0.9}(\nu_l/\nu_v)^{0.1}(\rho_l/\rho_v)^{0.5}$
h_{vl}	kJ/kg	evaporation enthalpy	η	Pa s	dynamic viscosity
k_{vs}	-	quality ratio $k_{vs} = \dot x_{eq} / \dot x_{act}$	λ	W/mK	heat conductance
$\dot m$	kg/m^2s	mass flux	ν	m^2/s	cinematic viscosity
M	-	molecular weight	ρ	kg/m^3	density
Pr	-	Prandtl number	ξ	-	friction fac. $\xi = (1.82\log_{10} Re - 1.64)^{-2}$
p_r	-	reduced pressure $p_r = p/p_{crit}$	$(\ )_v$		vapor
$\dot q$	W/m^2	heat flux	$(\ )_l$		liquid

6. ACKNOWLEDGMENT

The underlying work was carried out under contract from 'DLR (German Aerospace Research Establishment), Cologne/Stuttgart' within a cooperative project sponsored by the Federal German Ministry for Research and Technology.

7. REFERENCES

[1] Thome, J.: Flow Boiling in Horizontal Tubes: A Critical Assessment of Current Methodologies. Proc. Two-Phase Flow Modelling and Experimentation, eds. G.P. Celata, R.K. Shah, Vol. 1, pp. 41-52, 1995.

[2] Gungor, K.E. & Winterton, R.H.S.: A General Correlation for Flow Boiling in Tubes and Annuli, Int. J. Heat Mass Transfer, Vol. 29, pp. 351-358, 1986.

[3] Taitel, Y. & Dukler, A.E.: A Model for Predicting Flow Regime Transitions in Horizontal and Near Horizontal Gas-Liquid Flow, AIChE J., 22 (1), pp. 47-55, 1976.

[4] Herbst, O., Fechner, A., Köhler, W., Goebel, O. & Oberle, B.: Heat Transfer Behaviour of an Absorber Tube with Direct Steam Generation by Water Injection, Proc. Convective Flow Boiling Conference, ed.: J.C. Chen, Banff, Canada, 1995.

[5] Klug, F. & Mayinger, F.: Impedance Based Flow Reconstruction - A Novel Flow Composition Measuring Technique for Multi-phase Flows, Proc. NURETH-5 Meeting, Salt Lake City, Sept. 21-24, 1992.

[6] Gnielinski, V., Int. Chem. Eng., Vol. 6, pp. 359-368, 1976.